



Article

Effect of Sandy Soil Partial Replacement by Construction Waste on Mechanical Behavior and Microstructure of Cemented Mixtures

Diego Manchini Milani ¹, José Wilson dos Santos Ferreira ^{2,*}, Michéle Dal Toé Casagrande ³, Avacir Casanova Andrello ⁴ and Raquel Souza Teixeira ¹

¹ Department of Civil Construction, State University of Londrina, Londrina 86057-970, Paraná, Brazil

² Department of Civil Construction, Federal University of Technology—Paraná, Campo Mourão 87301-899, Paraná, Brazil

³ Department of Civil and Environmental Engineering, University of Brasília, Brasília 70910-900, Federal District, Brazil

⁴ Department of Physics, State University of Londrina, Londrina 86057-970, Paraná, Brazil

* Correspondence: jwferreira@utfpr.edu.br or wilson_s.ferreira@hotmail.com



Citation: Milani, D.M.; Ferreira, J.W.D.S.; Casagrande, M.D.T.; Andrello, A.C.; Teixeira, R.S. Effect of Sandy Soil Partial Replacement by Construction Waste on Mechanical Behavior and Microstructure of Cemented Mixtures. *Sustainability* **2022**, *14*, 12438. <https://doi.org/10.3390/su141912438>

Academic Editors: Michael Wistuba, Di Wang, Chiara Riccardi, Libo Yan, Zhanping You, Lily Poulikakos and Ana Jiménez del Barco Carrión

Received: 26 August 2022

Accepted: 26 September 2022

Published: 29 September 2022

Publisher's Note: MDPI stays neutral with regard to jurisdictional claims in published maps and institutional affiliations.



Copyright: © 2022 by the authors. Licensee MDPI, Basel, Switzerland. This article is an open access article distributed under the terms and conditions of the Creative Commons Attribution (CC BY) license (<https://creativecommons.org/licenses/by/4.0/>).

Abstract: The large amounts of construction waste (CW) generated yearly and its high landfilled proportion worldwide motivate the search for sustainable solutions. Thus, the effect of sandy soil partial replacement for construction waste in cemented mixtures was assessed in the present work in terms of mechanical behavior and microstructure. Distinct cement contents, compaction efforts, and curing periods were evaluated from soil-waste proportion of S75W25, S50W50, and S25W75. Tests of unconfined compression strength (UCS), indirect tensile strength (ITS), ultrasonic pulse velocity, water absorption, mercury intrusion porosimetry (MIP), and scanning electron microscopy (SEM) were conducted. The presence and increase in the amounts of cement and construction waste increase the optimum moisture content of the mixture. In contrast, only the CW content significantly affects maximum dry density. Both S75W25 and S50W50 mixtures resulted in similar UCS and ITS values, which was proven to be statistically equal by analysis of variance (ANOVA) at a 0.05 significance level, favoring CW replacing soil up to 50%. MIP and SEM results explained the sharp mechanical behavior transition obtained in 75% of CW. Cementation reactions resulted in macropores peak reduction and/or peak area translation to the left of the horizontal axis of the PSD curve, while its translation to the right indicates the cement mainly acting as filler, which was supported by SEM tests.

Keywords: recycling; mechanical properties; microstructure; sustainability; construction waste

1. Introduction

Generated by one of the most relevant economic sectors around the world, civil construction waste (CW) causes severe socio-environmental impacts. Globally, more than 10 billion tons of CW are produced yearly. China yields about 2.3 billion tons, the United States contributes over 700 million tons, and the European Union engenders more than 800 million tons [1–3]. Although CW generation in Brazil is much less than in the countries mentioned above, at approximately 44.5 million tons per year, comparing performance indicators with those countries has shown poor construction waste management [4,5].

In many countries, landfill is the primary treatment for waste generated from the construction industry, as illustrated by the United Kingdom (44%), Australia (44%), and Brazil (40%) [6]. Worldwide, the average construction waste landfilled is estimated to be around 35% [3]. Besides the low rate, this scenario indicates the need for integrated management since the material can be reused in the production chain, increasing the useful life of landfills, and it motivates the search for solutions toward sustainable development [1,7–9].

The recycling and posterior incorporation of construction waste in engineering applications is an effective alternative to move forward. CW in construction can collaborate to reduce

raw materials consumption, environmental impacts, land space occupation, energy and non-energy resources consumption, landfill depletion, and air, soil, and water pollution [10–13].

Several researchers indicate that CW aggregate has a great potential to be reused in engineering works, for example, recycled coarse aggregate for concrete production [14–18], backfilling material [19–21], and pavement layering [22–31].

The properties of construction waste are highly affected by the geological resources and the local construction technology, requiring physical, chemical, and mechanical characterization where the material is collected to assess its potential for use [32]. Leite et al. [31] investigated the feasibility of applying construction waste in pavements from its geotechnical characterization and mechanical behavior. They identified that the compaction process promoted a partial crushing and breakage of the aggregate, which contributed to an improvement in densification and, consequently, the bearing capacity, resilient modulus, and permanent deformation.

Arulrajah et al. [33–35] conducted an extensive experimental program to characterize distinct types of construction waste materials for pavement application. Their experimental program revealed the viability of recycled concrete aggregate, waste rock, and crushed brick. Similarly, the potential for stabilizing construction waste with cement kiln dust, fly ash, polymers, and recycled plastic was investigated by the authors [36–38]. Through compaction, California Bearing Ratio (CBR), and resilient modulus (RM) essays, similar feasibility was reported by Esfahani [26], who used a mixture of natural aggregate and CW. Cabalar et al. [25] enhanced unconfined compression strength by adding clay in recycled concrete aggregate, although the UCS results were only adequate for road pavement subgrade.

Based on previous experience in improving natural soil support capacity and mechanical behavior with cementing agents [39–43], researchers have investigated distinct combinations of these agents in mixtures of soil and CW [24,29,44]. Hasan et al. [44] conducted a series of UCS to evaluate the effect of ground granulated blast furnace slag and construction waste on stabilizing bentonite clay. They found an optimum proportion of 5% slag and 20% construction waste. Lukiantchuki et al. [29] partially replaced lateritic soil with construction waste in fiber-reinforced cement mixtures, leading to better geotechnical performance compared to natural soil.

Notwithstanding the advantages reported by the current studies, few works have explored the microstructural effect of CW incorporation in cemented soils and its mechanical response. Thus, the work aims to assess the feasibility of sandy soil partial replacement by CW in cemented mixtures. The current research contributes to explaining the interactions of the construction waste residue in cemented mixtures from a microstructural point of view and its effects on macro behavior, proposing a viable solution to sustainable applications in engineering.

2. Materials and Methods

2.1. Materials

The current experimental study was accomplished using sandy soil, construction waste, and Portland cement (Figure 1).

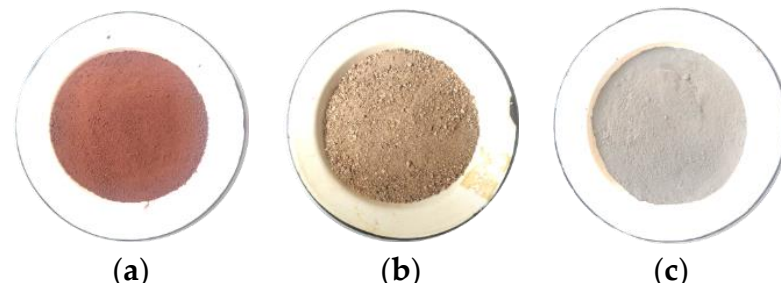


Figure 1. Materials used in this research: (a) sandy soil; (b) construction waste; (c) Portland cement.

The soil used in this research, clayey sand, was extracted near Federal Highway BR-487, northwest of the state of Paraná, Brazil ($23^{\circ}48'50.3''S$, $52^{\circ}59'58.8''W$, 410-m altitude). The chemical characterization of X-ray fluorescence indicated the presence of Si (48.7%), Al (27.7%), Fe (19.5%), and Ti (3.2%), following the mineral composition identified through X-ray diffraction, which mainly consisted of quartz (SiO_2), iron oxide (Fe_2O_3), and kaolinite ($Al_2Si_2O_5(OH)_4$). Additionally, the soil presented specific gravity of 2.89, liquid limit of 24.5%, and plasticity index of 10.0%, agreeing with previous works [45–48].

The construction waste was collected from a recycling site in Londrina, in the state of Paraná, Brazil. It is mainly composed of Ca (38.2%), Si (24.5%), and Fe (22.6%) from ceramic products, as well as concrete and cementitious mortar, presenting a specific gravity of 2.45. The CW water absorption was 21.50% due to the high specific area caused by the smaller particle size and the interconnected voids resulting from the cement paste attached to the surface of the aggregate particles [10,49].

Portland cement of high initial strength (Type III) was used as the cementing agent, presenting specific gravity of 3.24 [50]. Distilled water was used to characterize and homogenize the mixtures during the compaction process.

The particle-size distributions of clayey sand (S100) and construction waste (W100) are presented in Figure 2 [51,52]. The grain size distribution of the mixtures is shown based on soil and waste proportions of 25/75, 50/50, and 75/25.

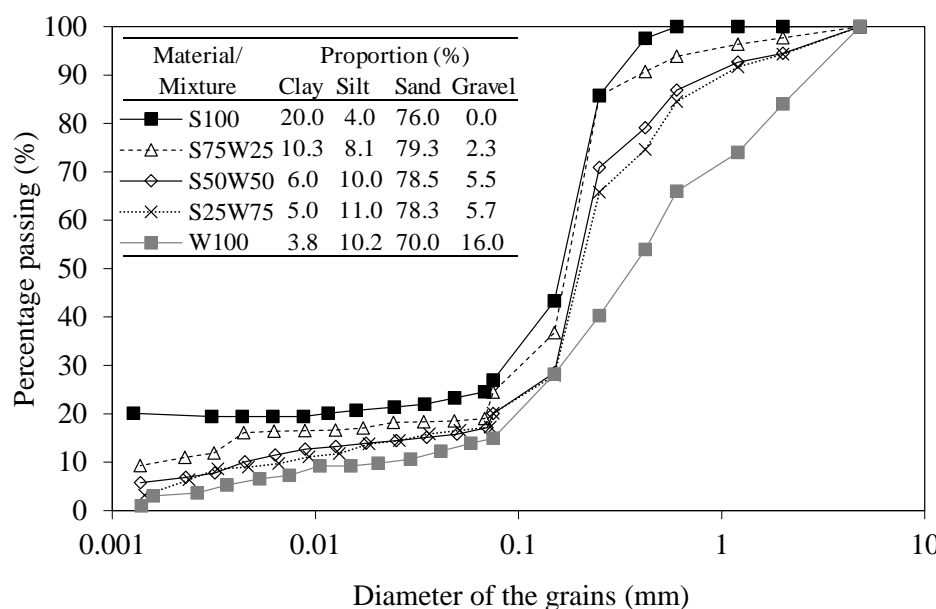


Figure 2. Particle-size distribution curve of the natural soil (S100), construction waste (W100), and mixtures (S75W25, S50W50, and S25W75).

According to the Unified Soil Classification System (USCS) and American Association of State Highway and Transportation Officials (AASHTO), the soil can be classified as clay sand (SC) and it belongs to group A-2-4.

2.2. Specimen Preparation

Samples with cement contents of 8%, 10%, and 12%, in relation to the dry mass of soil-CW, were used. The maximum dry density ($\rho_{d\ max}$) and optimum moisture content (ω_{opt}) for natural soil, soil-CW, and soil-CW-cement were defined by Proctor compaction tests under standard ($600\ kJ/m^3$) and modified ($2700\ kJ/m^3$) efforts, SE and ME, respectively [53,54].

It is noteworthy that particle breakage was not evaluated in this work, although the same procedure was employed in all conditions, intended to eliminate bias between the results. Similarly, it is believed that the soil matrix can reduce the potential breakage effect in soil-CW and soil-CW-cement mixtures.

The experimental conditions investigated and the average pH of each material/mixture are demonstrated in Table 1 [55]. It is essential to mention that the cement addition altered the acidic character presented by the natural tropical soil to an alkaline environment, favoring the cement chemical reactions [56].

Table 1. Experimental conditions investigated in the current study.

Material/Mixture	pH	Soil (%)	Waste (%)	Cement (%)
S100	5.27	100	0	0
S75W25	8.85	75	25	0
S50W50	10.29	50	50	0
S25W75	11.05	25	75	0
W100	11.23	0	100	0
S75W25C8	11.98	75	25	8
S75W25C10	12.24	75	25	10
S75W25C12	12.31	75	25	12
S50W50C8	12.40	50	50	8
S50W50C10	12.52	50	50	10
S50W50C12	12.65	50	50	12
S25W75C8	12.50	25	75	8
S25W75C10	12.59	25	75	10
S25W75C12	12.73	25	75	12

Specimens of 105-millimeter height and 50-millimeter diameter were prepared and compacted for mechanical tests based on the maximum dry density and optimum moisture content. Samples with compacting degree tolerances of $100 \pm 2\%$ and optimum moisture content variations ($\Delta\omega$) of $\pm 1.0\%$ were wrapped in waterproof plastic and stored in a wet room at a temperature of 23 ± 2 °C and air relative humidity equal to or greater than 95%. The curing periods were 7 and 28 days.

2.3. UCS and ITS

Unconfined compression strength (UCS) tests for compacted natural soil and mixtures were conducted following the ASTM D 2166 [57], in triplicate, under standard and modified efforts (Figure 3). After the curing stage, the mixtures were immersed in water for 4 h to assure a high saturation degree and decrease the suction effects on mechanical results. The test occurred under a controlled deformation of 1.27 mm/min.

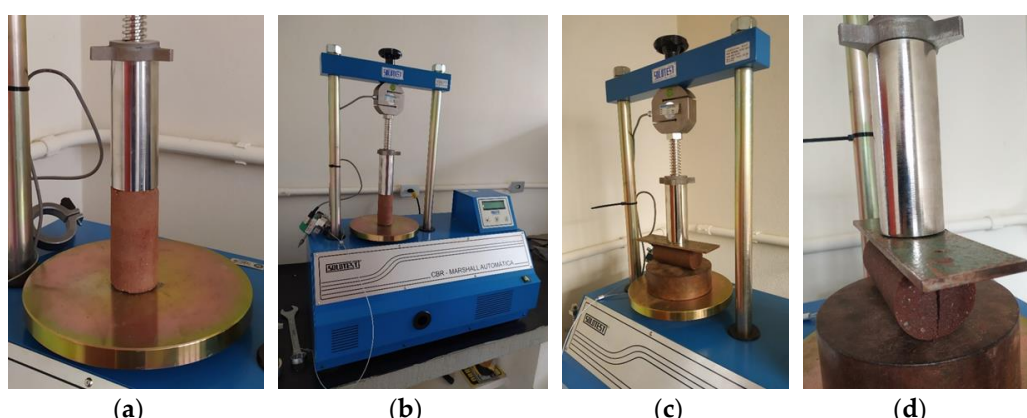


Figure 3. Mechanical testing of UCS and ITS: (a) specimen; (b) UCS test; (c) ITS test; (d) detail of equipment adaptation.

The indirect tensile strength (ITS) for both energy efforts was assessed per the Brazilian test method [58]. Tests were performed following a similar procedure as used for UCS tests, with two repetitions per experimental condition. It is important to emphasize that no difference was observed in previous tests to verify the accuracy between the ITS results obtained

in a universal testing machine and those obtained by the adaptation made (Figure 3d). The same procedure was verified and performed by other researchers [59,60].

As an acceptance criterion for UCS and ITS tests, it was established that the strength of the replicates, molded with the same characteristics, should not deviate more than 10% from the average strength.

2.4. Ultrasonic Tests

Ultrasonic tests were performed using Pundit Lab equipment in specimens referred to as the ITS since the tests are nondestructive (Figure 4). The test measures the ultrasonic pulse velocity (P-wave) emitted and received through two transducers (emitter/receptor) located on opposing faces of the specimen—via direct transmission. Before testing, the equipment was calibrated as follows: transducer frequency of 54 kHz, pulse width automatically adjusted, and a correction factor of 1 (standard recommended by the manufacturer), according to ASTM C 597 [61].

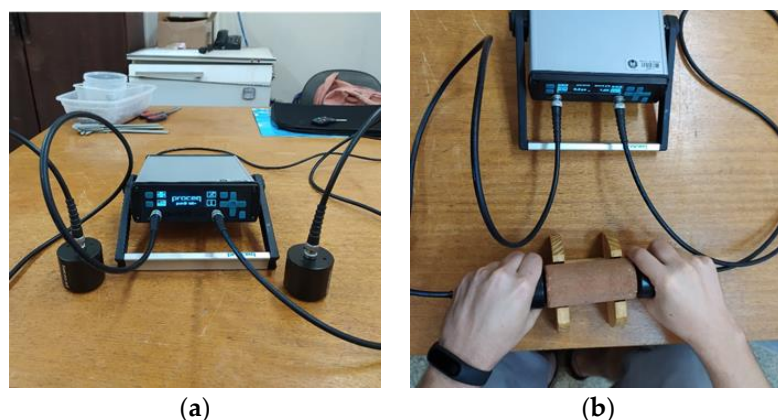


Figure 4. Ultrasonic test: (a) equipment; (b) execution.

To minimize the effects of refraction and reflection of the ultrasonic pulse occasioned by the presence of air between the surfaces of the sample and transducer, a fine layer of industrial gel was applied on both surfaces prior to testing [60].

2.5. Microstructural Tests

Microstructural analyses assessed the cementation and voids distribution by construction waste in the medium. The specimens used in scanning electron microscopy (SEM) and mercury intrusion porosimetry (MIP) were broken into small fragments after the UCS test and they were dried before the SEM and MIP tests (Figure 5).

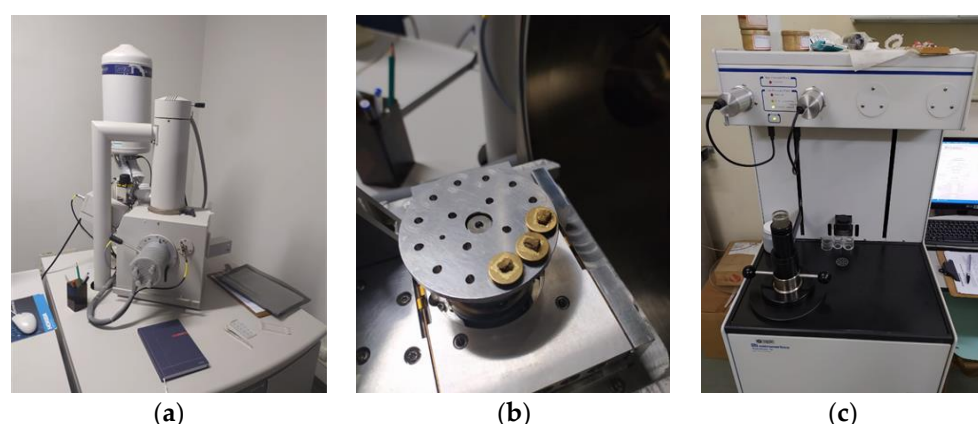


Figure 5. Microstructural tests: (a) SEM equipment; (b) specimen; (c) MIP equipment.

The SEM tests were conducted on the specimens of soil–CW–cement mixture molded under modified compaction effort and presented a fixed cement amount of 10% with a curing period of 28 days. An FEI-QUANTA 200 electronic microscope was used with an accelerating voltage of 25 kV. The small samples were sprayed with gold to become conductive and allow the analysis.

Besides natural soil and soil–CW samples, specimens of soil–CW–cement with 8% and 12% at 28 days of curing, under both compaction efforts, were tested in an automated AutoPore V MIP, with a pressure range from 0.1 to 60,000 Psia. The tests were conducted according to ASTM D 4404 [62].

3. Results and Discussion

3.1. Compaction Parameters

The average results for maximum dry density ($\rho_{d\ max}$) and optimum moisture content (ω_{opt}), considering the standard (600 kJ/m^3) and modified (2700 kJ/m^3) efforts, are presented in Figure 6 for natural soil, construction waste, soil–CW, and soil–CW–cement mixtures.

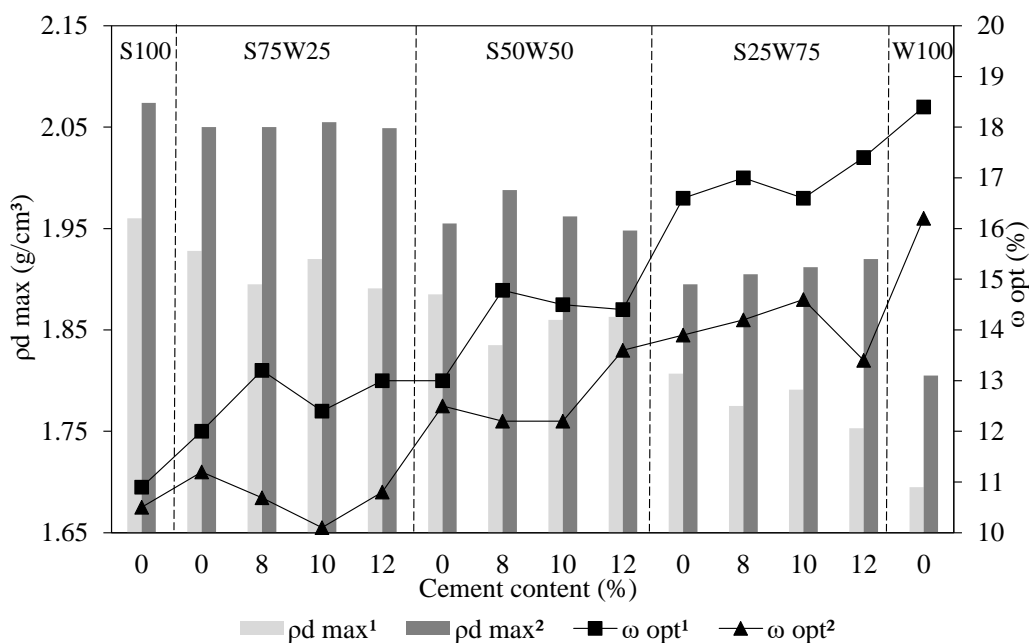


Figure 6. Compaction parameters for the natural soil, construction waste, and mixtures at standard and modified compaction efforts. ¹ standard compaction effort and ² modified compaction effort.

In general, adding CW to soil decreases the maximum dry density and increases the optimum moisture content, regardless of the compaction effort. The decrease in maximum dry density is due to the low specific gravity of construction waste compared with the soil. In contrast, the optimum moisture content increase is associated with the high amount of water absorption of recycled aggregate.

The cementing agent contributes to increasing the surface to be hydrated, demanding more water [24,59]. Regarding the maximum dry density, the cement addition has no significant effect, which was also reported by Lukiantchuki et al. [29]. Thus, the same trend can be observed for the results in both compaction efforts. Nevertheless, the modified effort generates a more densified structure, leading to higher maximum dry densities, and consequently, it reduces the void volume and the optimal moisture content.

3.2. UCS and ITS

The effect of construction waste incorporation on the unconfined compressive strength (UCS) and indirect tensile strength (ITS) of the soil is presented in Figure 7. As shown, both UCS and ITS decreased while CW content increased, except the ITS values for the mixture

S75W25. When comparing the same experimental conditions, the increase in compaction effort leads to higher UCS and ITS results.

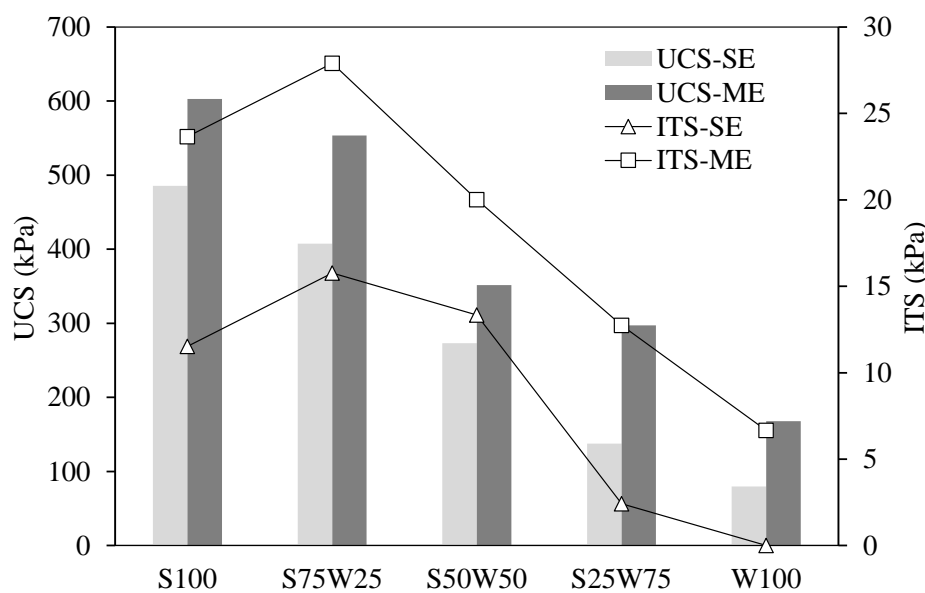


Figure 7. UCS and ITS of the compacted natural soil, CW, and uncemented mixtures.

For the soil–CW proportion of 75/25, it is believed that the increase in the percentage of coarse grains and the clay portion reduction do not compromise the mixture's structural arrangement. For the 50/50 proportion, it is assumed that CW increases the voids in the mixture and that the continuous decline in the clay portion also decreases the bonding between the materials, which affects the resistance, as Cabalar et al. [25] observed when using construction and demolition materials with clay soil.

The analysis conducted to evaluate the influence of partial soil replacement by CW on the mechanical behavior of cemented mixtures is presented in Figure 8.

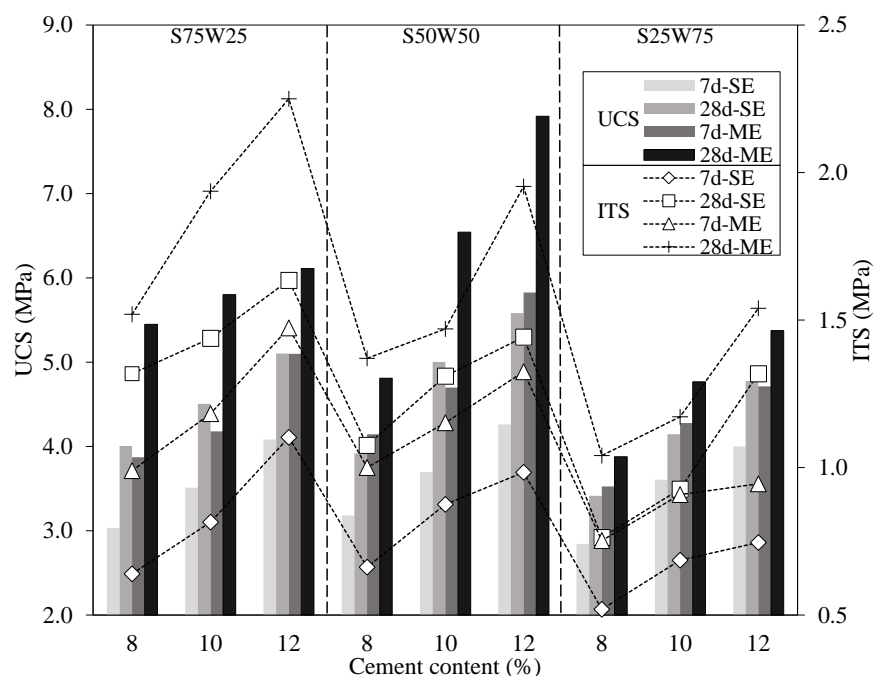


Figure 8. UCS and ITS of the cemented mixtures at 7 (7 d) and 28 days (28 d) of curing, using standard and modified compaction effort, SE and ME, respectively.

The cement addition developed a substantial improvement on both strength parameters studied. The UCS values for cemented mixtures were about 4.9 times higher (S25W75C8, 7 d, ME) and 12.1 times higher (S50W50C12, 28 d, ME) than the compacted natural soil. Considering the ITS, the gains were 30.8 (S25W75C8, 7 d, ME) and 140.9 times higher than the compacted soil (S75W25C12, 28 d, SE). From this analysis, it is possible to imply that the soil–CW–cement solution is more efficient in improving the soil tensile strength behavior, therefore, becoming a viable alternative for geotechnical applications, such as pavement layering [24–26,29].

The increases in cement content and compaction effort resulted in increments of UCS and ITS in all experimental conditions. It is important to note that cemented mixture S25W75 showed a reduction in the parameters when analyzed for other mixtures, indicating a limitation on the CW proportion.

Due to the similarity of unconfined compression strength and indirect tensile strength values between the S75W25- and S50W50-cemented mixtures, a variance analysis (ANOVA) at the significance level (α) of 0.05 was conducted, comparing the set of values for the same compaction effort and curing age. The p -values obtained for all statistical analyses were higher than 0.05 (Table 2), indicating the averages are statistically equal.

Table 2. Analysis of variance (ANOVA) of the UCS and ITS of cemented mixtures with soil-CW proportion of 75-25 and 50-50.

Compaction Effort	Curing Age (Days)	Factor	<i>p</i> -Value
SE	7	$UCS_{S75W25C}:UCS_{S50W50C}$	0.7107
	28		0.6393
ME	7		0.4551
	28		0.5268
SE	7	$ITS_{S75W25C}:ITS_{S50W50C}$	0.9544
	28		0.2482
ME	7		0.7682
	28		0.3305

Hereupon, soil replacements for CW up to 50% are more suitable for the experimental conditions evaluated in this study since they promote greater use of construction waste without significant losses on mechanical properties compared to the S75W25-cemented mixture. Therefore, they provide a technical and socio-environmental solution to the problems associated with residue disposal and natural resources exploration.

3.3. UPV and Water Absorption

The P-wave velocity and water absorption (WA) for soil–CW–cement mixtures are shown in Figure 9, considering the standard and modified efforts, and curing periods of 7 and 28 days. It is essential to highlight that water absorption is related to the partial filling of inter-aggregate open pores with water and it does not include the intra-agglomerate micropores.

It is well-established that cemented mixture S75W25 resulted in superior values of p-wave velocity, which is related to a denser mixture. Conversely, the water absorption was lower for this mixture, showing good agreement of inversely proportional results.

As the construction waste proportion increases, the p-wave decreases, indicating the voids in the mixtures are increasing. The wave does not propagate through the mixture voids; thus, the increase in voids reduces the velocity. On the other hand, when interconnected, these voids result in greater water absorption, as indicated in Figure 9. Both compaction energy increment and cement content addition tend to lower this effect through cement hydration products and the pozzolanic reaction that occurs during the curing period.

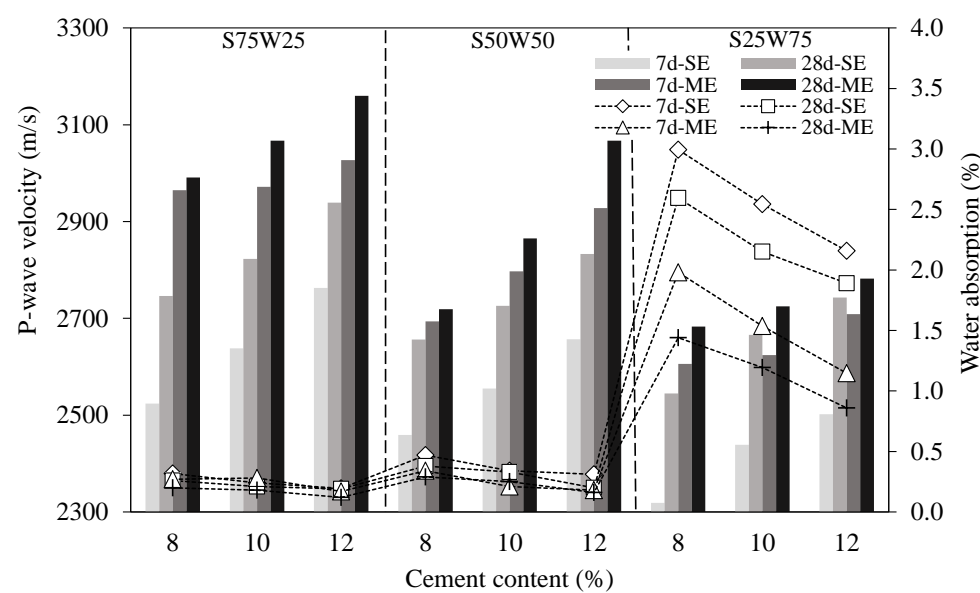


Figure 9. P-wave velocity and water absorption values of cemented mixtures, considering distinct curing periods (7 and 28 days) and compaction efforts (standard and modified).

Figure 10 shows the relation between indirect tensile strength and p-wave velocity, considering standard (Figure 10a) and modified (Figure 10b) efforts. The linear correlations obtained (R^2 0.72) demonstrated that the incorporation of construction waste in the mixtures did not affect the well-established trend presented by cemented soils [60,63–66].

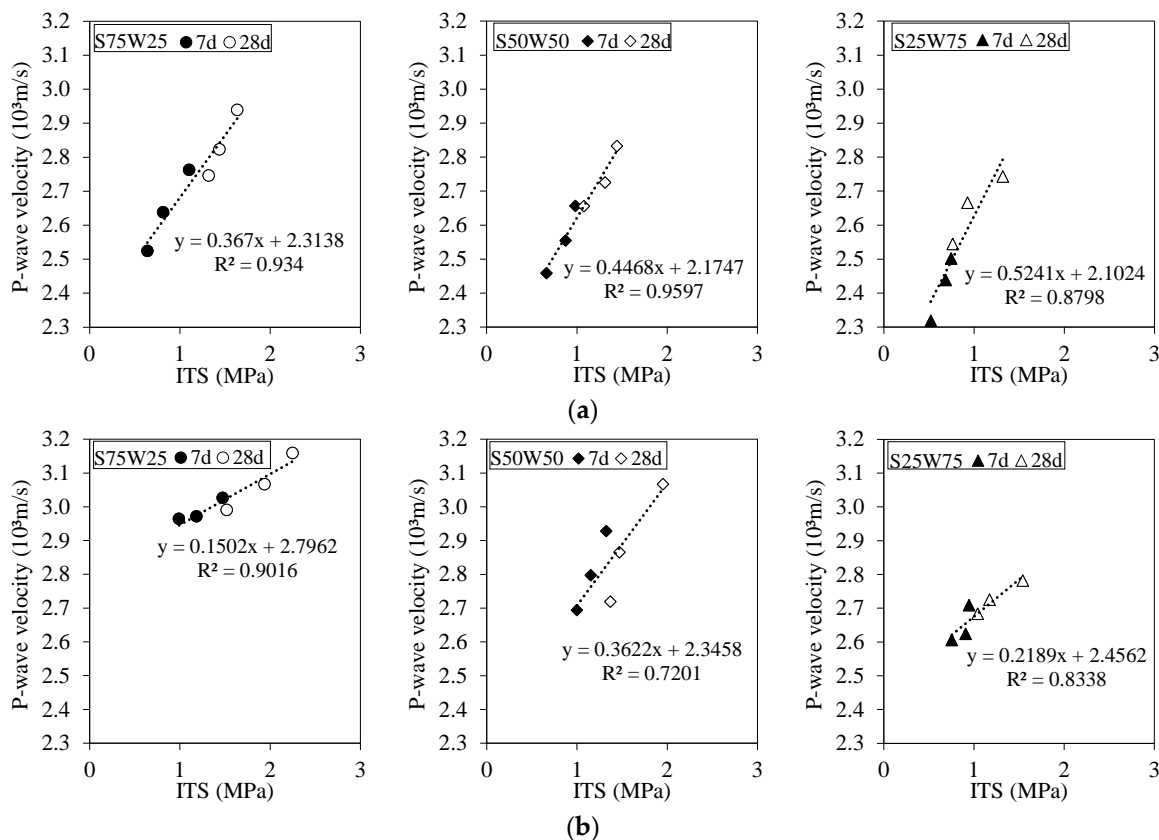


Figure 10. Relation between ITS and p-wave velocity for the cemented mixtures with soil and CW proportion of 25/75, 50/50, and 75/25, considering: (a) standard compaction effort—SE; (b) modified compaction effort—ME.

The construction waste addition causes an increase in the slopes of the curves for mixtures compacted at standard effort (Figure 10a), which demonstrates that increasing the amount of residue significantly impacts the mechanical behavior of the mixture.

The slope reduction in the tendency line for the modified energy compaction (Figure 10b) indicates a smaller p-wave variation for this experimental condition. As velocity is a measurement associated with both densification and voids distribution in the mixture, compaction can be seen as the main factor affecting the p-wave. On the other hand, the cementation effect is noticed in the ITS behavior.

3.4. Pore Size Distribution

The improvement in mechanical behavior for soil–CW mixtures by the compaction effort and cement hydration products can be seen through the pore size distribution (PSD) of MIP tests (Figure 11), considering standard and modified compaction effort, SE and ME, respectively.

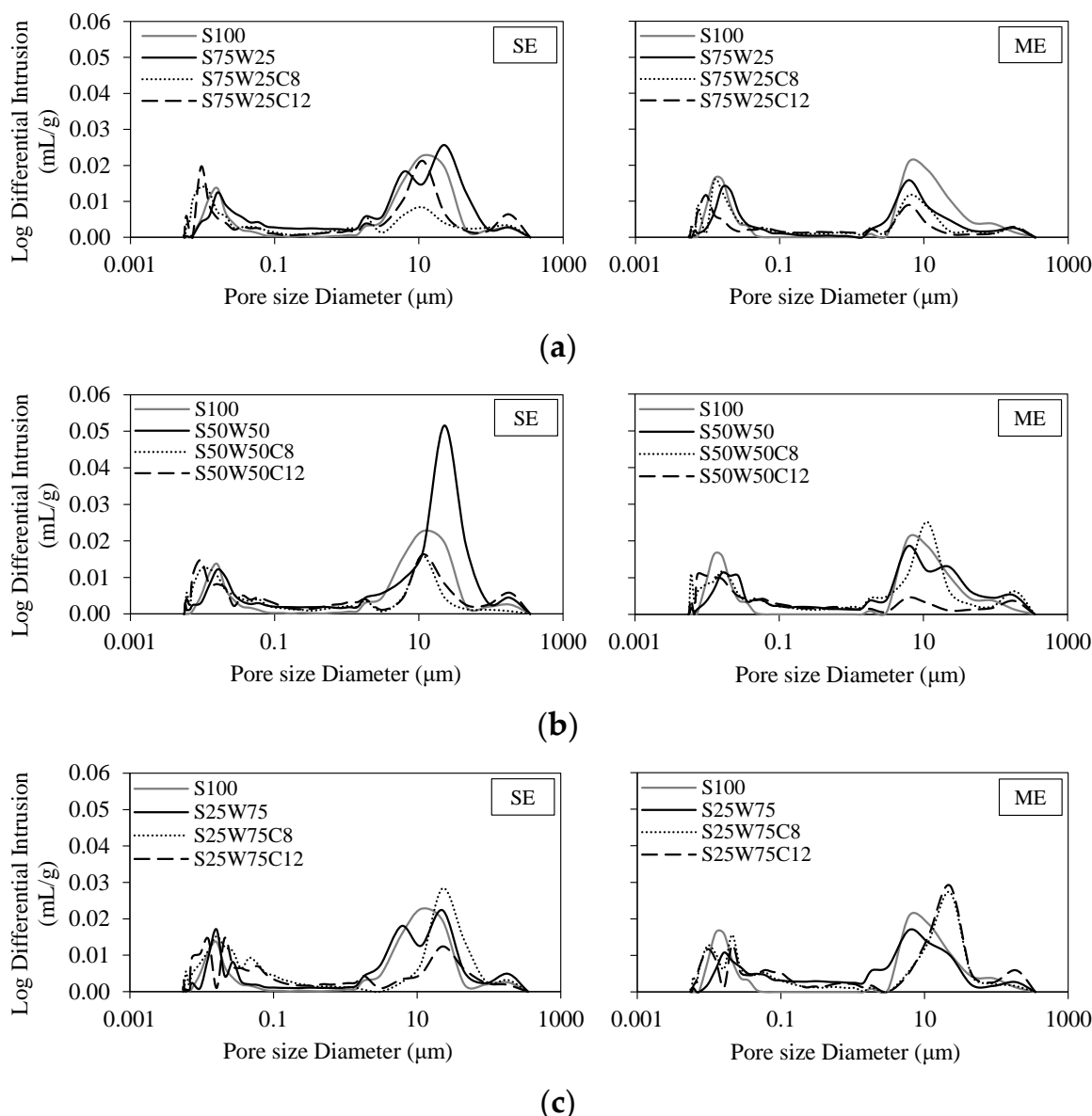


Figure 11. Pore size distribution of natural soil, soil–CW, and soil–CW–cement, at standard (SE) and modified compaction efforts (ME) for the mixtures: (a) S75W25; (b) S50W50; (c) S25W75.

In general, the CW incorporation in the soil resulted in growth in the peak areas for SE. At the same time, the increment in the compaction energy reduced the pore growth sensibility for CW addition. The S75W25 mixture compacted at ME indicated pore closure for natural soil (Figure 11a), which reasonably explains the similarity between UCS values and the improvement of ITS by S75W25 when compared to compacted natural soil.

Independently on the compaction effort and the cement presence and amount, the pore size distribution tendency is bimodal and approximately concentrated at $0.003\text{ }\mu\text{m}$ and $10\text{ }\mu\text{m}$. The class of pore diameters in these peak regions may be attributed to intra-agglomerate micropores and inter-agglomerate macropores, respectively, prevailing the macropores. From this perspective, the increase in CW proportion tends to elevate the peaks for uncemented mixtures.

The cement acts on the reduction in frequency and width at the peak regions, mainly in inter-agglomerate macropores, as observed by Lemaire et al. [42]. For the same compaction effort, an increase in the amount of cement leads to a decrease in the peaks, since more cementing agent is available to perform primary and secondary chemical reactions.

The exception to this behavior occurred for the soil–CW–cement mixtures with a soil and CW proportion of 25/75 (Figure 11c), using ME, in which the cement addition increased pore size and peak in the macropore region, translating this area to the right of the horizontal axis.

The S25W75 proportion increased the mixture pore size, reducing the cement reaction effects and resulting in voids filling as the main contribution, which is proven through the overlapping curves of S25W75C8 and S25W75C12 mixtures in the modified energy. Because cement is a very thin material, its effect occurs on the void adjacent surface, narrowing the macropore strip width, as the curve shape shows in Figure 11c.

In a simplified approach, the translation of the peak to the left and/or its reduction in the inter-agglomerate macropores region can be understood as a cementation effect, as there is a reduction in the number of pores or the pore size is reducing. In contrast, the translation of the peak to the right in the pore size diameter axis indicates the cement is mainly acting as filler.

3.5. Microstructural Images by SEM

SEM images were taken from the soil–CW–cement mixtures with 28 days of curing (Figure 12). A dense structure is seen in the mixture S75W25C10 (Figure 12a), in which the soil texture is modified and considerably covered by cement hydration products and pozzolanic reaction, as calcium silicate hydrate crystal (C-S-H), calcium hydroxide (CH), and ettringite (Aft), forming a netted structure that spans broad zones.

The same products from hydration and pozzolanic reactions on a smaller scale are observed in mixtures S50W50C10 (Figure 12b), indicating the construction waste rise affects the aggregates surface coverage and bonding by the reticulate and fibrous structure of CSH, CH, and ettringite, which increases the volume of pores.

Especially in S25W75C10 (Figure 12c), it is possible to observe a weakly packed and more porous structure compared to the other mixtures. Regardless of the cementitious products identified in its structure, larger pores prevent the formation of a netted structure and, therefore, negatively affect the mechanical behavior. Further, it is necessary to clarify that a part of the voids in the mixture is the result of intrinsic porosity in the old cement pastes from the recycled aggregate [10,16], in which the effect is expected to be more significant on S25W75C10 due to its higher CW proportion.

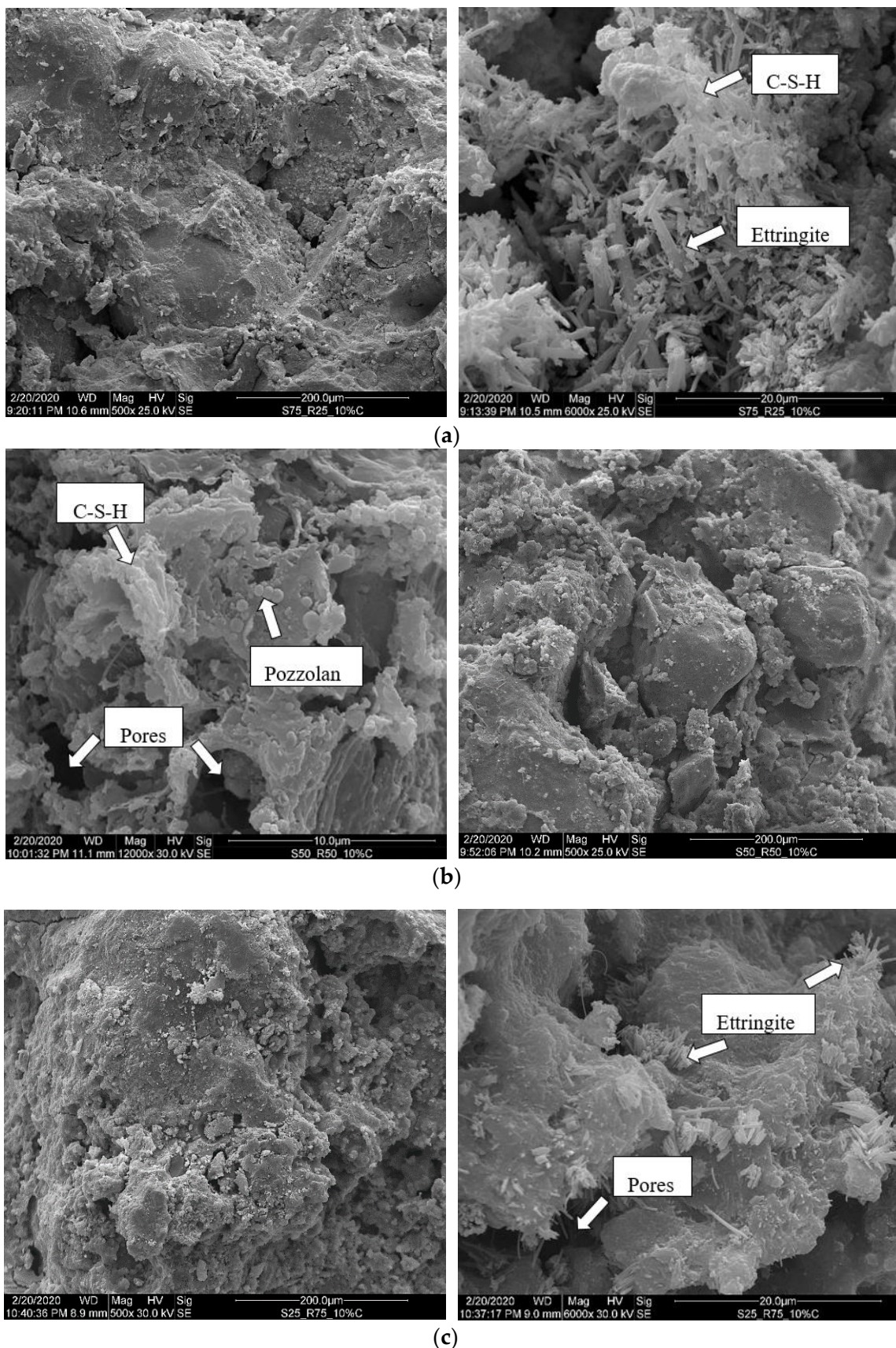


Figure 12. SEM tests for cemented mixtures at 10% cement, 28 days of curing, ME, considering: (a) S75W25; (b) S50W50; (c) S25W75.

4. Conclusions

From the results and analyses presented in this paper, it is possible to conclude that:

- The optimum moisture content of the mixtures was affected by both the presence and increase in the amounts of construction waste and cement, while only the CW content contributed to significant differences in maximum dry density.
- The improvement in mechanical behavior by cement is more evident in indirect tensile strength (30.8–140.9 times higher) than unconfined compressive strength (4.9–12.1 times higher). Thus, cemented soil-waste mixtures demonstrate viable applications, such as pavement layers.
- From 75% CW in the mixture, a limitation in the improvements is observed due to the reduction in cementation effects.
- UCS and ITS of S75W25- and S50W50-cemented mixtures proved to be statistically identical. Therefore, the mix with 50% of construction waste is most suitable, since it advances the use in civil applications.
- The results of p-wave velocity and ITS show satisfactory correlation, demonstrating the cemented mixtures with CW insertion follow the established trend of cemented soils.
- The natural soil, soil-CW, and soil-CW-cement mixtures presented a bimodal tendency in pore size distribution. Both increases in cement amount and compaction effort resulted in pore closure, reflecting in UCS and ITS gains.
- The peak reduction located in the macropores region on the PSD curves and/or translation of this region to the left of the horizontal axis indicates the occurrence of cement hydration products and pozzolanic reaction. On the other hand, its translation to the right reflects the performance of cement as a filler in general.

Based on the experimental program limitations, future studies could explore the following: investigating lower cement levels, replacing soil with residues of distinct compositions, and evaluating other cementing agents.

Author Contributions: Conceptualization, D.M.M., J.W.d.S.F. and R.S.T.; methodology, J.W.d.S.F.; formal analysis, D.M.M. and J.W.d.S.F.; investigation, D.M.M. and R.S.T.; resources, R.S.T., A.C.A. and M.D.T.C.; data curation, J.W.d.S.F.; writing—original draft preparation, J.W.d.S.F.; writing—review and editing, J.W.d.S.F.; supervision, R.S.T. and M.D.T.C. All authors have read and agreed to the published version of the manuscript.

Funding: This research was funded by National Council for Scientific and Technological Development—CNPq, grant number 2018 426100/2018-2, and 141127/2019-8, and by the Coordination for the Improvement of Higher Level or Education Personnel—CAPES—grant number 23038.003556/2020-88.

Institutional Review Board Statement: Not applicable.

Informed Consent Statement: Not applicable.

Data Availability Statement: The data used are available to the corresponding author upon request.

Acknowledgments: The authors acknowledge the support provided by the State University of Londrina (UEL) and the University of Brasilia (UnB).

Conflicts of Interest: The authors declare no conflict of interest.

References

1. Zheng, L.; Wu, H.; Zhang, H.; Duan, H.; Wang, J.; Jiang, W.; Dong, B.; Liu, G.; Zuo, J.; Song, Q. Characterizing the generation and flows of construction and demolition waste in China. *Constr. Build. Mater.* **2017**, *136*, 405–413. [[CrossRef](#)]
2. Wu, H.; Zuo, J.; Zillante, G.; Wang, J.; Yuan, H. Status quo and future directions of construction and demolition waste research: A critical review. *J. Clean. Prod.* **2019**, *240*, 118163. [[CrossRef](#)]
3. Chen, K.; Wang, J.; Yu, B.; Wu, H.; Zhang, J. Critical evaluation of construction and demolition waste and associated environmental impacts: A scientometric analysis. *J. Clean. Prod.* **2021**, *287*, 125071. [[CrossRef](#)]
4. ABRELPE Panorama of Waste in Brazil 2020. *Brazilian Assoc. Public Clean. Spec. Waste ABRELPE 2020*. Available online: <https://abrelpe.org.br/panorama-2020/> (accessed on 25 August 2022).
5. Nunes, K.R.A.; Mahler, C.F. Comparison of construction and demolition waste management between Brazil, European Union and USA. *Waste Manag. Res.* **2020**, *38*, 415–422. [[CrossRef](#)]

6. Kabirifar, K.; Mojtabaei, M.; Wang, C.; Tam, V.W.Y. Construction and demolition waste management contributing factors coupled with reduce, reuse, and recycle strategies for effective waste management: A review. *J. Clean. Prod.* **2020**, *263*, 121265. [[CrossRef](#)]
7. Maués, L.M.F.; do Nascimento, B.D.M.O.; Lu, W.; Xue, F. Estimating construction waste generation in residential buildings: A fuzzy set theory approach in the Brazilian Amazon. *J. Clean. Prod.* **2020**, *265*, 121779. [[CrossRef](#)]
8. Cristiano, S.; Ghisellini, P.; D'Ambrosio, G.; Xue, J.; Nesticò, A.; Gonella, F.; Ulgiati, S. Construction and demolition waste in the Metropolitan City of Naples, Italy: State of the art, circular design, and sustainable planning opportunities. *J. Clean. Prod.* **2021**, *293*, 125856. [[CrossRef](#)]
9. Negash, Y.T.; Hassan, A.M.; Tseng, M.-L.; Wu, K.-J.; Ali, M.H. Sustainable Construction and Demolition Waste Management in Somaliland: Regulatory Barriers lead to Technical and Environmental Barriers. *J. Clean. Prod.* **2021**, *297*, 126717. [[CrossRef](#)]
10. Behera, M.; Bhattacharyya, S.K.; Minocha, A.K.; Deoliya, R.; Maiti, S. Recycled aggregate from C&D waste & its use in concrete—A breakthrough towards sustainability in construction sector: A review. *Constr. Build. Mater.* **2014**, *68*, 501–516. [[CrossRef](#)]
11. Akanbi, L.A.; Oyedele, L.O.; Akinade, O.O.; Ajayi, A.O.; Davila Delgado, M.; Bilal, M.; Bello, S.A. Salvaging building materials in a circular economy: A BIM-based whole-life performance estimator. *Resour. Conserv. Recycl.* **2018**, *129*, 175–186. [[CrossRef](#)]
12. dos Santos Ferreira, J.W.; Senez, P.C.; Casagrande, M.D.T. Pet Fiber Reinforced Sand Performance Under Triaxial and Plate Load Tests. *Case Stud. Constr. Mater.* **2021**, *15*, e00741. [[CrossRef](#)]
13. dos Santos Ferreira, J.W.; Marroquin, J.F.R.; Felix, J.F.; Farias, M.M.; Casagrande, M.D.T. The feasibility of recycled micro polyethylene terephthalate (PET) replacing natural sand in hot-mix asphalt. *Constr. Build. Mater.* **2022**, *330*, 127276. [[CrossRef](#)]
14. Sagoe-Crentsil, K.K.; Brown, T.; Taylor, A.H. Performance of concrete made with commercially produced coarse recycled concrete aggregate. *Cem. Concr. Res.* **2001**, *31*, 707–712. [[CrossRef](#)]
15. Etxeberria, M.; Vázquez, E.; Marí, A.; Barra, M. Influence of amount of recycled coarse aggregates and production process on properties of recycled aggregate concrete. *Cem. Concr. Res.* **2007**, *37*, 735–742. [[CrossRef](#)]
16. Thomas, C.; Setién, J.; Polanco, J.A.; Alaejos, P.; Sánchez De Juan, M. Durability of recycled aggregate concrete. *Constr. Build. Mater.* **2013**, *40*, 1054–1065. [[CrossRef](#)]
17. Moretti, J.P.; Sales, A.; Almeida, F.C.R.; Rezende, M.A.M.; Gromboni, P.P. Joint use of construction waste (CW) and sugarcane bagasse ash sand (SBAS) in concrete. *Constr. Build. Mater.* **2016**, *113*, 317–323. [[CrossRef](#)]
18. Costa, F.N.; Ribeiro, D.V. Reduction in CO₂ emissions during production of cement, with partial replacement of traditional raw materials by civil construction waste (CCW). *J. Clean. Prod.* **2020**, *276*, 123302. [[CrossRef](#)]
19. Santos, E.C.G.; Palmeira, E.M.; Bathurst, R.J. Behaviour of a geogrid reinforced wall built with recycled construction and demolition waste backfill on a collapsible foundation. *Geotext. Geomembranes* **2013**, *39*, 9–19. [[CrossRef](#)]
20. Rahman, M.A.; Imteaz, M.; Arulrajah, A.; Disfani, M.M. Suitability of recycled construction and demolition aggregates as alternative pipe backfilling materials. *J. Clean. Prod.* **2014**, *66*, 75–84. [[CrossRef](#)]
21. Vieira, C.S.; Pereira, P.M.; Lopes, M.D.L. Recycled Construction and Demolition Wastes as filling material for geosynthetic reinforced structures. Interface properties. *J. Clean. Prod.* **2016**, *124*, 299–311. [[CrossRef](#)]
22. Sangiorgi, C.; Lantieri, C.; Dondi, G. Construction and demolition waste recycling: An application for road construction. *Int. J. Pavement Eng.* **2014**, *16*, 530–537. [[CrossRef](#)]
23. Cardoso, R.; Silva, R.V.; de Brito, J.; Dhir, R. Use of recycled aggregates from construction and demolition waste in geotechnical applications: A literature review. *Waste Manag.* **2015**, *49*, 131–145. [[CrossRef](#)] [[PubMed](#)]
24. Sharma, R.K.; Hymavathi, J. Effect of fly ash, construction demolition waste and lime on geotechnical characteristics of a clayey soil: A comparative study. *Environ. Earth Sci.* **2016**, *75*, 377. [[CrossRef](#)]
25. Cabalar, A.F.; Zardikawi, O.A.A.; Abdulnafaa, M.D. Utilisation of construction and demolition materials with clay for road pavement subgrade. *Road Mater. Pavement Des.* **2017**, *20*, 702–714. [[CrossRef](#)]
26. Esfahani, M.A. Evaluating the feasibility, usability, and strength of recycled construction and demolition waste in base and subbase courses. *Road Mater. Pavement Des.* **2018**, *21*, 156–178. [[CrossRef](#)]
27. Panizza, M.; Natali, M.; Garbin, E.; Tamburini, S.; Secco, M. Assessment of geopolymers with Construction and Demolition Waste (CDW) aggregates as a building material. *Constr. Build. Mater.* **2018**, *181*, 119–133. [[CrossRef](#)]
28. Sharma, A.; Sharma, R.K. Effect of addition of construction–demolition waste on strength characteristics of high plastic clays. *Innov. Infrastruct. Solut.* **2019**, *4*, 27. [[CrossRef](#)]
29. Lukiantchuki, J.A.; de Oliveira, J.R.M.D.S.; de Almeida, M.D.S.S.; dos Reis, J.H.C.; Silva, T.B.; Guideli, L.C. Geotechnical Behavior of Construction Waste (CW) as a Partial Replacement of a Lateritic Soil in Fiber-Reinforced Cement Mixtures. *Geotech. Geol. Eng.* **2020**, *39*, 919–942. [[CrossRef](#)]
30. Liu, L.; Li, Z.; Cai, G.; Liu, X.; Yan, S. Humidity field characteristics in road embankment constructed with recycled construction wastes. *J. Clean. Prod.* **2020**, *259*, 120977. [[CrossRef](#)]
31. Leite, F.D.C.; Motta, R.D.S.; Vasconcelos, K.L.; Bernucci, L. Laboratory evaluation of recycled construction and demolition waste for pavements. *Constr. Build. Mater.* **2011**, *25*, 2972–2979. [[CrossRef](#)]
32. Rodrigues, F.; Carvalho, M.T.; Evangelista, L.; De Brito, J. Physical-chemical and mineralogical characterization of fine aggregates from construction and demolition waste recycling plants. *J. Clean. Prod.* **2013**, *52*, 438–445. [[CrossRef](#)]
33. Arulrajah, A.; Piratheepan, J.; Aatheesan, T.; Bo, M.W. Geotechnical Properties of Recycled Crushed Brick in Pavement Applications. *J. Mater. Civ. Eng.* **2011**, *23*, 1444–1452. [[CrossRef](#)]

34. Arulrajah, A.; Piratheepan, J.; Disfani, M.M.; Bo, M.W. Geotechnical and Geoenvironmental Properties of Recycled Construction and Demolition Materials in Pavement Subbase Applications. *J. Mater. Civ. Eng.* **2013**, *25*, 1077–1088. [CrossRef]
35. Arulrajah, A.; Ghorbani, B.; Narsilio, G.; Horpibulsuk, S.; Leong, M. Thermal performance of geothermal pavements constructed with demolition wastes. *Geomech. Energy Environ.* **2021**, *28*, 100253. [CrossRef]
36. Arulrajah, A.; Yaghoubi, E.; Wong, Y.C.; Horpibulsuk, S. Recycled plastic granules and demolition wastes as construction materials: Resilient moduli and strength characteristics. *Constr. Build. Mater.* **2017**, *147*, 639–647. [CrossRef]
37. Arulrajah, A.; Mohammadinia, A.; D’Amico, A.; Horpibulsuk, S. Cement kiln dust and fly ash blends as an alternative binder for the stabilization of demolition aggregates. *Constr. Build. Mater.* **2017**, *145*, 218–225. [CrossRef]
38. Poltue, T.; Suddeepong, A.; Horpibulsuk, S.; Samingthong, W.; Arulrajah, A.; Rashid, A.S.A. Strength development of recycled concrete aggregate stabilized with fly ash-rice husk ash based geopolymers as pavement base material. *Road Mater. Pavement Des.* **2019**, *21*, 2344–2355. [CrossRef]
39. Consoli, N.C.; Foppa, D.; Festugato, L.; Heineck, K.S. Key Parameters for Strength Control of Artificially Cemented Soils. *J. Geotech. Geoenvir. Eng.* **2007**, *133*, 197–205. [CrossRef]
40. Consoli, N.C.; Cruz, R.C.; Floss, M.F.; Festugato, L. Parameters Controlling Tensile and Compressive Strength of Artificially Cemented Sand. *J. Geotech. Geoenvir. Eng.* **2010**, *136*, 759–763. [CrossRef]
41. Horpibulsuk, S.; Rachan, R.; Chinkulkijniwat, A.; Raksachon, Y.; Suddeepong, A. Analysis of strength development in cement-stabilized silty clay from microstructural considerations. *Constr. Build. Mater.* **2010**, *24*, 2011–2021. [CrossRef]
42. Lemaire, K.; Deneele, D.; Bonnet, S.; Legret, M. Effects of lime and cement treatment on the physicochemical, microstructural and mechanical characteristics of a plastic silt. *Eng. Geol.* **2013**, *166*, 255–261. [CrossRef]
43. Tongwei, Z.; Xibing, Y.; Yongfeng, D.; Dingwen, Z.; Songyu, L. Mechanical behaviour and micro-structure of cement-stabilised marine clay with a metakaolin agent. *Constr. Build. Mater.* **2014**, *73*, 51–57. [CrossRef]
44. Hasan, U.; Chegenizadeh, A.; Budihardjo, M.A.; Nikraz, H. Experimental Evaluation of Construction Waste and Ground Granulated Blast Furnace Slag as Alternative Soil Stabilisers. *Geotech. Geol. Eng.* **2016**, *34*, 1707–1722. [CrossRef]
45. Oliveira, A.D.D.; Pelaquim, F.G.P.; Zanin, R.F.B.; Melo, T.R.D.; Tavares Filho, J.; Andrello, A.C.; Teixeira, R.S. The structure of tropical lateritic soils as an impacting factor in the shape of soil-water characteristic curves. *Soils Rocks* **2022**, *45*, 1–13. [CrossRef]
46. Cancian, M.A.; Cancian, V.A.; Teixeira, R.S.; Fontenele, H.B.; Da costa Branco, C.J.M. Influência do teor de umidade, da porosidade e do intervalo de tempo até a aplicação da mistura solo-cimento em pavimento rodoviário. *Transportes* **2017**, *25*, 41–50. [CrossRef]
47. ASTM D 854; Standard Test Methods for Specific Gravity of Soil Solids by Water Pycnometer. ASTM International: West Conshohocken, PA, USA, 2014.
48. ASTM D 4318; Standard Test Methods for Liquid Limit, Plastic Limit, and Plasticity Index of Soils. ASTM International: West Conshohocken, PA, USA, 2017.
49. ABNT NBR NM 30; Fine Aggregate—Determination of Water Absorption. Associação Brasileira de Normas Técnicas: São Paulo, Brazil, 2001.
50. ASTM C 188; Standard Test Method for Density of Hydraulic Cement. ASTM International: West Conshohocken, PA, USA, 2017.
51. ASTM D 7928; Standard Test Method for Particle-Size Distribution (Gradation) of Fine-Grained Soils Using the Sedimentation (Hydrometer) Analysis. ASTM International: West Conshohocken, PA, USA, 2021.
52. ASTM D 6913; Standard Test Methods for Particle-Size Distribution (Gradation) of Soils Using Sieve Analysis. ASTM International: West Conshohocken, PA, USA, 2017.
53. ASTM D 698; Standard Test Methods for Laboratory Compaction Characteristics of Soil Using Standard Effort. ASTM International: West Conshohocken, PA, USA, 2021.
54. ASTM D 1557; Standard Test Methods for Laboratory Compaction Characteristics of Soil Using Modified Effort. ASTM International: West Conshohocken, PA, USA, 2021.
55. Pavan, M.A.; Bloch, M.F.; Zempulski, H.C.; Miyazawa, M.; Zocoler, D.C. *Manual de Análise Química do Solo e Controle de Qualidade*; IAPAR: Londrina, Brazil, 1992.
56. de Carvalho, J.C.; de Rezende, L.R.; Cardoso, F.B.D.F.; de FL Lucena, L.C.; Guimarães, R.C.; Valencia, Y.G. Tropical soils for highway construction: Peculiarities and considerations. *Transp. Geotech.* **2015**, *5*, 3–19. [CrossRef]
57. ASTM D 2166; Standard Test Method for Unconfined Compressive Strength of Cohesive Soil. ASTM International: West Conshohocken, PA, USA, 2016. [CrossRef]
58. ASTM D 3967; Standard Test Method for Splitting Tensile Strength of Intact Rock Core Specimens. ASTM International: West Conshohocken, PA, USA, 2016.
59. dos Santos Ferreira, J.W.; Casagrande, M.D.T.; Teixeira, R.S. Sample dimension effect on equations controlling tensile and compressive strength of cement-stabilized sandy soil under optimal compaction conditions. *Case Stud. Constr. Mater.* **2021**, *15*, e00763. [CrossRef]
60. Ferreira, J.; Casagrande, M.; Teixeira, R. Sample dimension effect on cement-stabilized sandy soil mechanical behavior. *Soils Rocks* **2022**, *45*, 1–10. [CrossRef]
61. ASTM C 597; Standard Test Method for Pulse Velocity Through Concrete. ASTM International: West Conshohocken, PA, USA, 2016. [CrossRef]
62. ASTM D 4404; Standard Test Method for Determination of Pore Volume and Pore Volume Distribution of Soil and Rock by Mercury Intrusion Porosimetry. ASTM International: West Conshohocken, PA, USA, 2018. [CrossRef]

63. Khan, Z.; Majid, A.; Cascante, G.; Hutchinson, D.J.; Pezeshkpour, P. Characterization of a cemented sand with the pulse-velocity method. *Can. Geotech. J.* **2006**, *43*, 294–309. [[CrossRef](#)]
64. Toohey, N.M.; Mooney, M.A. Seismic modulus growth of lime-stabilised soil during curing. *Geotechnique* **2012**, *62*, 161–170. [[CrossRef](#)]
65. Mandal, T.; Tinjum, J.M.; Edil, T.B. Non-destructive testing of cementitious stabilized materials using ultrasonic pulse velocity test. *Transp. Geotech.* **2016**, *6*, 97–107. [[CrossRef](#)]
66. Kutanaei, S.S.; Choobasti, A.J. Effects of Nanosilica Particles and Randomly Distributed Fibers on the Ultrasonic Pulse Velocity and Mechanical Properties of Cemented Sand. *J. Mater. Civ. Eng.* **2017**, *29*, 04016230. [[CrossRef](#)]